Numerical Methods in Civil Engineering, 6-2 (2021) 93-106

Numerical Methods in Civil Engineering

Journal Homepage: https://nmce.kntu.ac.ir/

Seismic Resilience Assessment of Tehran's Southern Water Transmission Pipeline Using GIS-based Analyses

Ali Shojaeian[*], Saeideh Farahani[**], Behrouz Behnam[***], and Mohammad Reza Mashayekhi[****]

ARTICLE INFO

RESEARCH PAPER

Article history:
Received:
April 2021.
Revised:
August 2021.
Accepted:
October 2021.

Keywords:
Infrastructure Resilience, GIS-based Analysis, Water Transmission Pipeline, Seismic Risk Assessment

Abstract:

It is well accepted that an urban region's seismic resilience is directly related to the seismic resilience of the local water systems. Pipelines having low earthquake resistance generally include old pipes and those susceptible to corrosion. The seismic vulnerability of the water transmission pipelines can be evaluated along with the geologic hazards such as landslides, liquefaction, fault movement, etc. In this study, GIS-based analyses are implemented for one of Tehran's main water transmission pipelines, which transfer Mamloo Dam water to Tehran's southern regions, by considering the four most probable earthquake scenarios to evaluate post-earthquake serviceability of the studied pipeline. Transient Ground Deformation (TGD) due to seismic wave propagation, and also Permanent Ground Deformation (PGD), which may result in liquefaction (lateral spreading, and ground settlement) and landslide, are regarded as destructive earthquake effects on the water transmission pipelines. A restoration curve is also developed for the worst scenario to investigate the adequate post-earthquake water supply throughout the service area and ensure rapid system recovery. Results show that the water serviceability index regarding the worst earthquake scenario (Rey fault activated) is 28%, which means that more than 72% of the study area's population will experience severe disruption of water availability in a potential earthquake.

1. Introduction

There is ample evidence that damage due to natural disasters such as earthquakes has increased in the world over the last decades. The concept of seismic resilience has gained significant attention in recent years to mitigate direct and indirect earthquake losses [1-3]. Iran's position on the Alpine-Himalayan seismic belt has put this country among one of the world's largest earthquake-prone countries in a way that, about 97% of Iran's cities and villages are located in seismic regions [4].

* *Ph.D. Student, School of Civil Engineering and Environmental Science, University of Oklahoma, Norman, USA.*
** *Ph.D., School of Civil and Environmental Engineering, Amirkabir University of Technology, Tehran, Iran.*
*** *Corresponding author: Assistant Professor, School of Civil and Environmental Engineering, Amirkabir University of Technology, Tehran, Iran. Email:* behrouz.behnam@uqconnect.edu.au
**** *Assistant Professor, Civil Engineering Department, K. N. Toosi University of Technology, Tehran, Iran.*

Investigation of previous earthquakes in Iran indicates that most of the sustained damage pertained to critical infrastructure, highlights the need to pay further attention to these facilities to prevent possible future physical damage [5]. Recently, several studies have addressed this need by investigating the seismic vulnerability and resilience of some of the lifeline systems in Iran [6-8].

To be more specific, supply, transmission, and distribution of water play an important role in the resilience of the urban regions. Urban water systems are considered as critical infrastructures as they are directly related to a society's vital need, and any interruption to their assigned functionalities can rapidly lead to a catastrophe with destructive consequences. The seismic resilience of an urban region (i.e., the ability to recover from an earthquake with the least amount of negative impacts) can be interconnected to the functionality of water transmission systems. Therefore, it is critical for water transmission systems to recover rapidly after an earthquake. As water transmission systems are not often designed to withstand

earthquake forces, there may hence sustain considerable damage during an earthquake. A detailed report on seismic loss estimation of water resource systems was released by ASCE in 1991 [9]. In this study, Peak Ground Acceleration (PGA)-based fragility relations were calculated using collected damage data by Katayama et al. [10] and the Coalinga pipeline damage in 1983. Fragility relation presented by O'Rourke and Ayala [11], was used in FEMA HAZUS-MH's loss assessment methodology [12]. After the Northridge earthquake in 1994, a GIS-based method was introduced by O'Rourke et al. [13] to examine various factors that can affect the Los Angeles Department of Water and Power (LADWP) and the Metropolitan Water District (MWD) water supply services. The fragility relations for pipelines were also assessed in terms of Modified Mercalli Intensity (MMI), PGA, and Peak Ground Velocity (PGV). O'Rourke et al. [13] concluded that the best-related factor to the pipeline damage is PGV; therefore, PGV-based fragilities were proposed for steel, Cast Iron (CI), Ductile Iron (DI), and Asbestos Cement (AC) pipelines. In another study, the American Lifeline Alliance (ALA) presented a set of algorithms to compute the probability of earthquake damage that affects various components of water supply systems [14]. Further analyses on water resources' pipeline damages were followed by Pineda-Porras and Ordaz-Schroeder [15] using the Michoacan earthquake data (1985) in Mexico City. A detailed PGV map was used to find the best relationship between repair rate and seismic intensity [16]. Rahnama et al. [17] assessed the seismic vulnerability of 11 primary water distribution networks in Tehran and indicated that all of the considered primary water distribution networks in Tehran would not face much damage, rather only some secondary parts might sustain damage.

This study aims at developing a GIS-based model with the ability to assess the seismic damage to pipelines for two major geological seismic hazards, including ground shaking and ground failure simultaneously. The model developed and used in this study includes four main parts of a database implementation, seismic hazard analysis, vulnerability assessment, and determining the pipeline's serviceability. While the model is independent of any specific case, it is employed for one of Tehran's main water transmission pipelines, which transfers the Mamloo Dam water to Tehran's southern regions; by regarding four probable earthquake scenarios.

2. Method of Approach

In this study various parameters, such as PGA, PGV, and Permanent Ground Displacement (PGD), are calculated to determine the seismic vulnerability of water transmission pipelines. GIS-based analyses are performed to evaluate the post-earthquake serviceability of the studied pipeline. Also, a recovery curve is developed for the worst scenario to investigate the adequate post-earthquake water supply throughout the service area and ensure rapid system recovery.

The methodology for the step by step analysis is presented in detail, as shown in Fig. 1. The used framework consists of the following steps: 1) investigating of site condition, 2) estimating permanent and transient ground deformations, 3) determining pipelines damages, 4) evaluating the serviceability index, and 5) calculating the backup water resources. Fig. 1 presents a flow diagram showing a summary of the framework employed in this study. In summary, HAZUS methodology is used for estimating the permanent and transient ground deformation due to potential earthquakes. Then, pipelines damage rates are estimated to evaluate the number of leaks and breaks that would happen in the length of the pipeline. The outcome is used to determine the serviceability index and backup water resources needed during the repair process. All the mentioned steps are clarified in the next section.

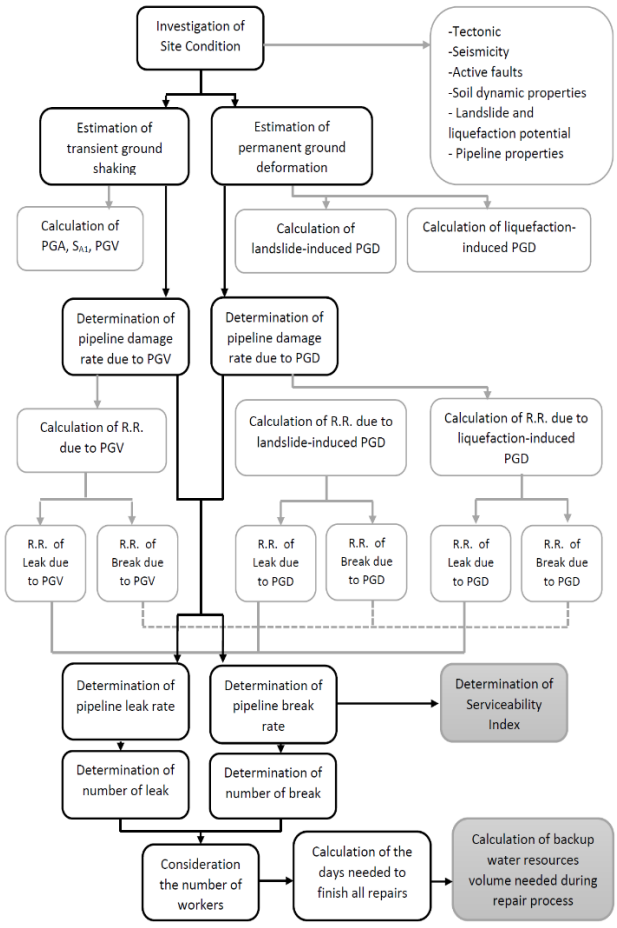

Fig. 1: Flowchart for evaluating the performance of water transmission systems.

3. Case Study

Tehran, the capital city of Iran, has a population of over 8.7 million. The most important water resources in Tehran are Karaj, Lar, Latian, Mamloo, and Taleghan reservoirs. Mamloo Dam reservoir is located on the Jajrood River, about 45 km from east of Tehran. The studied region is located between 32-35 northern latitude and 38-52 eastern longitude of the equator, a part of Tehran Province regarding the country's divisions. The building of this dam was to take advantage of the capacity of the catchment area of Jajrood River and supply the agricultural water of Varamin and Pakdasht and part of the daily needs of Tehran. The type of construction used in the Mamloo Dam is soiled with a clay core, and the reservoir volume is 250 m^3 [18].

Tehran is situated on the southern foothills of the Alborz Mountains, which is an east-west trending mountain range with a 600 km length and 100 km width along the Alpine Himalayan seismic belt. Tectonically, Alborz is an active zone under tremendous tectonic stresses due to the northward convergence of central Iran toward Eurasia. At Tehran's longitude, Alborz accommodates 6–10 mm of shortening per year [19-21]. As a result of such active tectonics, Tehran is surrounded by several major faults, embracing some inner-city active faults. These faults mainly show both reverse and strike-slip mechanisms. Here is a brief description of some of the most important active faults inside or in Tehran's vicinity, along with their main specific features [22, 23]. Also, details of the fault model parameters, which are obtained from the JICA study, are summarized in Table 1 [24].

- North Tehran: The most prominent active tectonic structure in Tehran; E–W strike; north-dipping fault surface; length of 175 km with a predominant thrust mechanism along its 110–km western segment, and a predominant left-lateral strike-slip mechanism along its 65-km eastern segment; average slip rate of ~0.3 mm yr^{-1}.
- Mosha: Located at 16–km distance to the north of Tehran; N100° E trending; north-dipping fault surface; a 220–km long, left-lateral oblique reverse fault with dips varying from 35° to 50°; average slip rate of ~0.2 mm yr^{-1}.
- Parchin: Also known as the Eyvanekey fault; situated at the southeast of Tehran; 70 km long; NW–SE strike; has clear ruptures in Quaternary alluvial deposits.
- Rey: A zone located south of Tehran, E–W trending, consisting of Kahrizak, South Rey, and North Rey faults with lengths of 35, 18.5, and 16.5 km, respectively.

3.1. Seismic Hazard Analyses

The first earthquake effect, which can damage lifelines and infrastructure, is Transient Ground Deformation (TGD) due to seismic wave propagation. The second one is Permanent Ground Deformation (PGD), which may result in liquefaction (lateral spreading and ground settlement), landslide, and ground failure. For risk assessment of lifelines and infrastructure as broadened over the country, investigating TGD and PGD is of vital importance. In this study, PGD is first calculated and mapped using the HAZUS methodology [12]. Thereafter, by separating the water transmission pipeline into small segments of 1000 m (to neglect behavior/property variability along with the segments and subsequently increase the accuracy of analyses), the outputs of the hazard analyses are assigned to each segment. The main reasons for pipelines' segmentation are to accurately consider the geotechnical seismic hazards that varied continuously in each small region [25].

3.1.1. Hazard analyses of ground shaking (seismic wave passage)

TGD caused by seismic waves generated during an earthquake is transient vibratory soil deformation, which is considered a wave passage effect covering broad geographic areas and affects pipelines in different soil types. As proposed in HAZUS, for obtaining PGV, the first step is to calculate the spectral acceleration by having a soil classification of a region in terms of dynamic properties. According to the ShakeMap [26] method, for areas lacking Vs30 maps, including most of the globe, the approach of [27], which provides estimations of Vs30 as a function of more available topographic slope data can be employed. In this study, soil classification is carried out using a topographic gradient map, and the global 1-arcsecond (30-m) SRTM digital elevation model (DEM) of Iran is used for producing a slope map. The soil classification map is then produced, and PGV is inferred from 1-s spectral acceleration using Equation (1).

$$PGV = (\frac{386.4}{2\pi}.S_{A1})/1.65 \quad (1)$$

where S_{A1} is the spectral acceleration in the 1-s period. Therefore, the induced-PGV map of the studied water transmission pipeline is prepared according to four earthquake scenarios, as shown in Fig. 3.

Table 1. Fault model parameters of four important active faults considered in the current study [24].

Scenario	Fault	Length (km)	Width (km)	Magnitude(M_w)	Origin		Azimuth (Clockwise from North) (degrees)	Dip angle (degrees)
					Longitude	Latitude		
1	North-Tehran	58	27	7.2	52.4955	35.6815	263	75
2	Mosha	68	30	7.2	51.5061	35.5876	283	75
3	Rey	26	16	6.7	51.7392	35.8255	263	75
4	Parchin	27	28	6.9	51.773	35.494	296	50

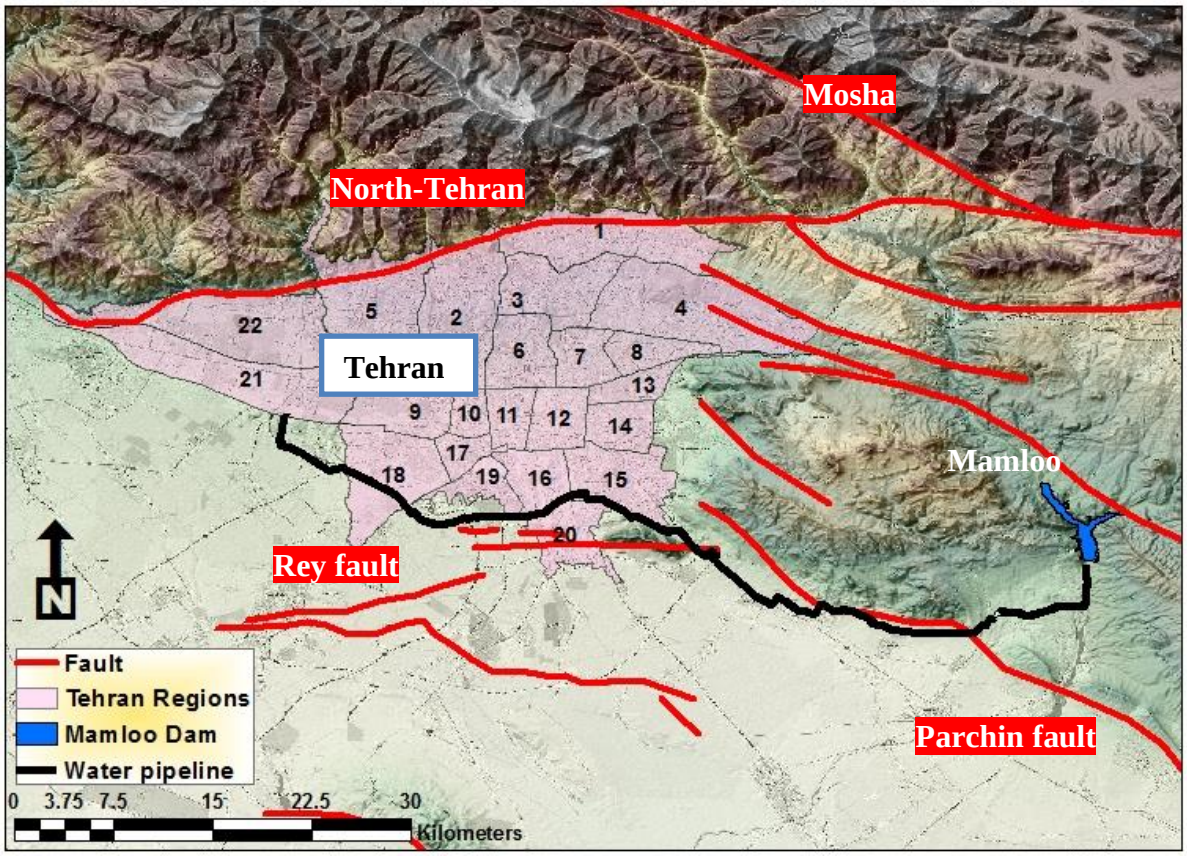

Fig. 2: The studied region map

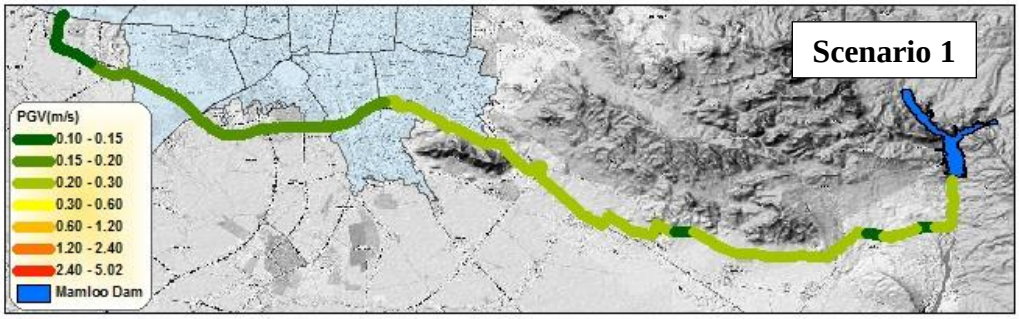

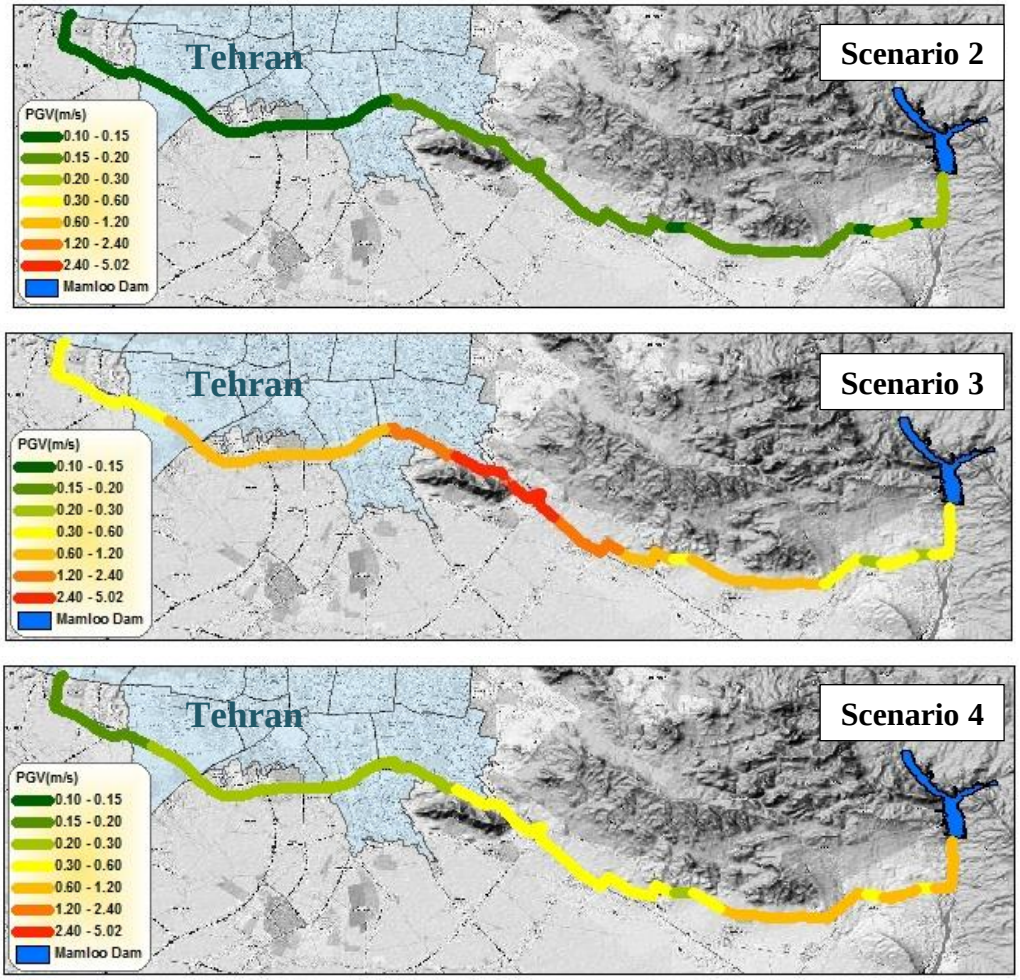

Fig. 3: PGV contours of the pipeline for different scenarios.

3.1.2. Hazard analyses of ground failure

The ground failures caused by such geotechnical seismic phenomena as liquefaction (lateral spreading and ground settlement) and landslide are localized in particular prone geographic zones. Liquefaction is the most critical hazard due to ground failure that can threaten infrastructure. Liquefaction is a soil behavior phenomenon in which a saturated soil loses a substantial amount of strength due to excessive pore-water pressure generated by and accumulated during strong earthquake ground shaking [12]. Permanent ground displacements due to lateral spreading and differential settlement are commonly considered as significant potential hazards associated with liquefaction. In this study, to consider the failure caused by soil liquefaction, the Iran liquefaction susceptibility map is used. This map is provided by the International Institute of Earthquake Engineering and Seismology (IIEES) and is based on previous studies performed by Komakpanah [28]. Based on the HAZUS methodology, the probability of liquefaction for a given susceptibility category can be determined using Equation 2:

$$P[Liquifaction] = \frac{P[Liquifaction|PGA = pga]}{K_M K_W} P_{ml} \quad (2)$$

where $P[Liquifaction|PGA = pga]$ is the conditional liquefaction probability for a given susceptibility category at a specified level of PGA, K_M is the moment magnitude correction factor, K_W is the groundwater correction factor, and Pml is the proportion of the susceptible map unit. The expected value of lateral spreading-induced PGD conditioned to the occurrence of liquefaction can be stated as a function of PGA [29]. It is assumed that ground settlement associated with liquefaction is related to the susceptibility category assigned to an area. This assumption is consistent with the relationship presented by Tokimatsu and Seed [30] that indicates strong correlations between volumetric strain (settlement) and soil relative density as a measure of susceptibility. Therefore, the expected settlement at a location is the product of the probability of liquefaction as presented in Equation 2 for a given ground motion level and the characteristic settlement amplitude appropriate to the susceptibility category. The map of liquefaction-induced PGD of the studied water transmission pipeline is presented in Fig. 4 regarding the four considered earthquake scenarios.

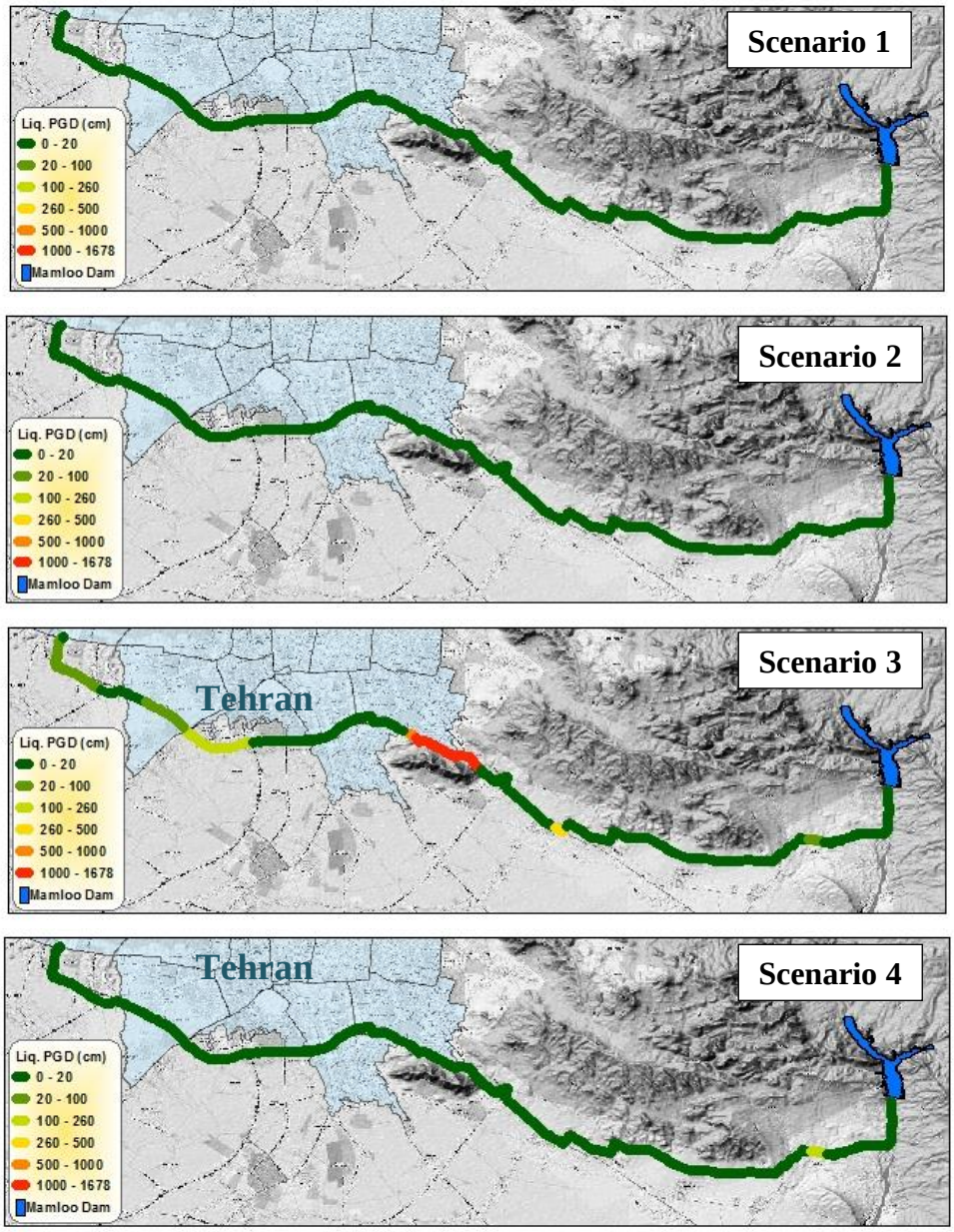

Fig. 4: Liquefaction-induced PGD contours of the pipeline for different scenarios.

Earthquake-induced landslide of a hillside slope occurs when the static plus inertia forces within the slide mass cause the factor of safety to drop below 1.0 temporarily. The value of PGA within the slide mass required to cause the factor of safety to drop to 1.0 is denoted by the critical or yield acceleration (ac). This acceleration value is determined based on pseudo-static slope stability analyses and/or empirically based on observations of slope behavior during past earthquakes. The landslide hazard evaluation requires the characterization of a region's landslide susceptibility or sub-regions soil/geologic conditions. For this purpose, the Iran landslide susceptibility map, provided by the Geological Survey of Iran [31], and critical acceleration at any location proposed by HAZUS for susceptibility categories are used. The permanent ground displacements are determined using Equation. (3):

$$E[PGD] = E\left[{}^{d}/_{a_{is}}\right] a_{is} n \quad (3)$$

where $E\left[{}^{d}/_{a_{is}}\right]$ is the expected displacement factor, a_{is} is the induced acceleration (in a decimal fraction of g's), and n is the number of cycles. A relation derived from the results of Makdisi and Seed [32] is used to calculate downslope displacements. Based on HAZUS, at any given location, there is a specified probability of having a landslide susceptible deposit, and that landsliding either occurs or does not occur within susceptible deposits depending on whether the induced peak ground acceleration exceeds the critical acceleration. Hence, the landslide occurrence probability is achieved using Table 2. The map of landslide-induced PGD of the studied water transmission pipeline is presented in Fig. 5 for the considered scenarios.

Table 2: Percentage of Map Area Having a Landslide-Susceptible Deposit [12]

Susceptibility Category	None	I	II	III	IV	V	VI	VII	VIII	IX	X
Map Area	0.00	0.01	0.02	0.03	0.05	0.08	0.10	0.15	0.20	0.25	0.30

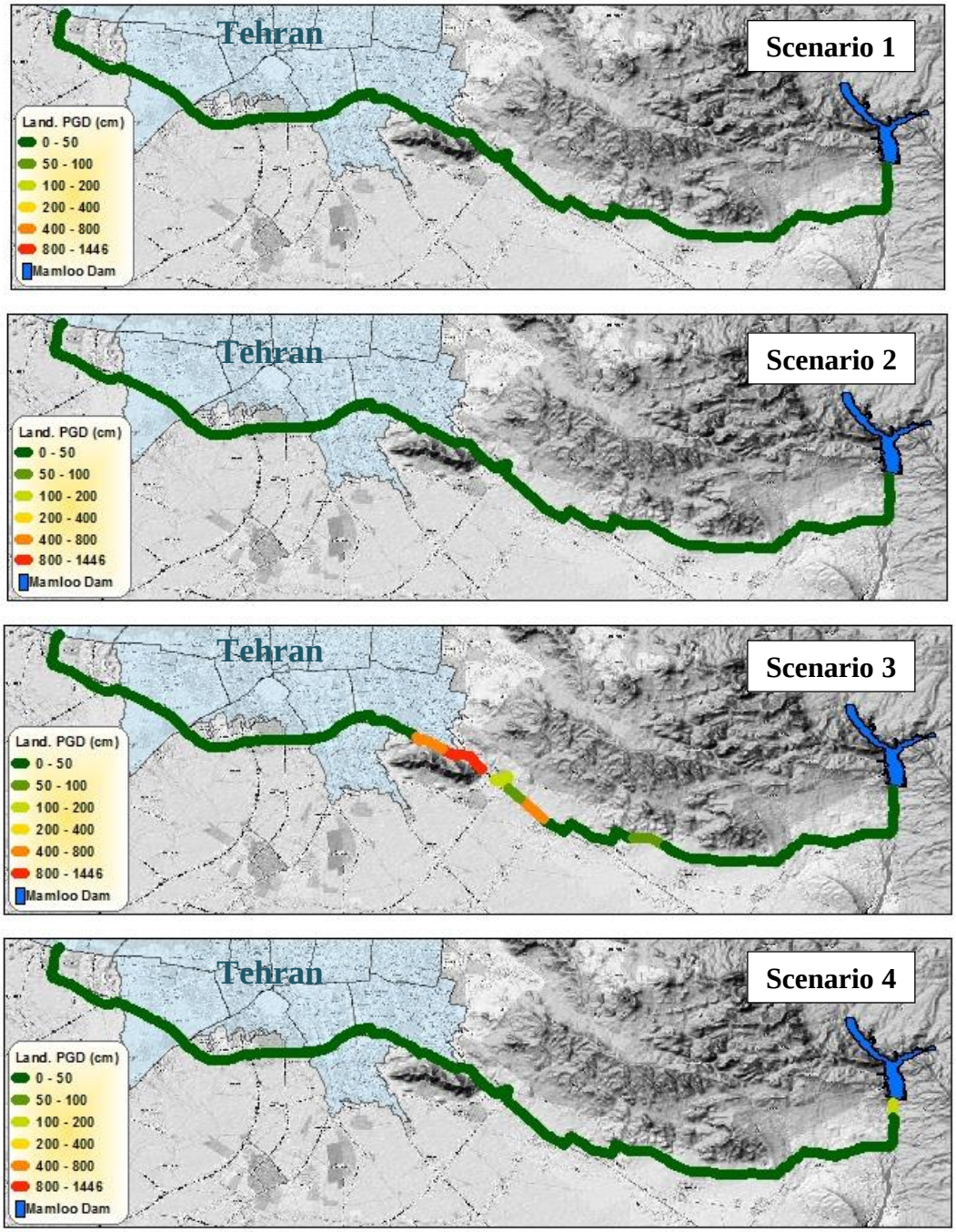

Fig. 5: Landslide-induced PGD contours of the pipeline for different scenarios.

3.2. Damage Assessment

For pipelines, two damage states are considered; these are leaks and breaks. Generally, when a pipe sustains damage due to ground failure (PGD), the type of damage is likely a break, while when a pipe sustains damage due to seismic wave propagation (PGV), the type of damage is likely a joint pull-out or crushing at the bell. The loss methodology assumes that damage due to seismic waves will consist of 80% leaks and 20% breaks, while damage due to ground failure will consist of 20% leaks and 80% breaks.

The vulnerability functions, which relate overall pipe damage measures to relatively simple demand intensity descriptions, are entirely empirical relationships that express the pipeline expected failure as a function of

seismic parameters of strong ground motion. These functions, which are presented based on reported damage from historical earthquakes, express the pipeline's seismic damages as Repair Rate (RR) per unit length of pipe. RR can be explained as a rate between the number of repairs and the length [km] of a pipe exposed to seismic hazards, which mainly includes TGD and PGD caused by Strong Ground Shaking (SGS) and Ground Failure (GF), respectively. Different damage sources (SGS and GF), materials, joint, and diameter of pipes are taken into account to provide damage functions (Equations (4) and (5)) by the ALA [14] to calculate the RR.

$$R.R_{SGS} = K_1.0.002416.PGV \quad (4)$$

$$R.R_{GF} = K_2.11.223.PGD^{0.319} \quad (5)$$

where, for example, K_1 and K_2 for continuous iron pipelines are both 0.15. According to the hazard analysis section results and using Equations 4 and 5, the RR maps are accordingly produced. Fig. 6 shows the maps of the number of leaks due to the PGV and PGD. Also, Fig. 7 shows the break maps due to the PGV and PGD for the considered scenarios.

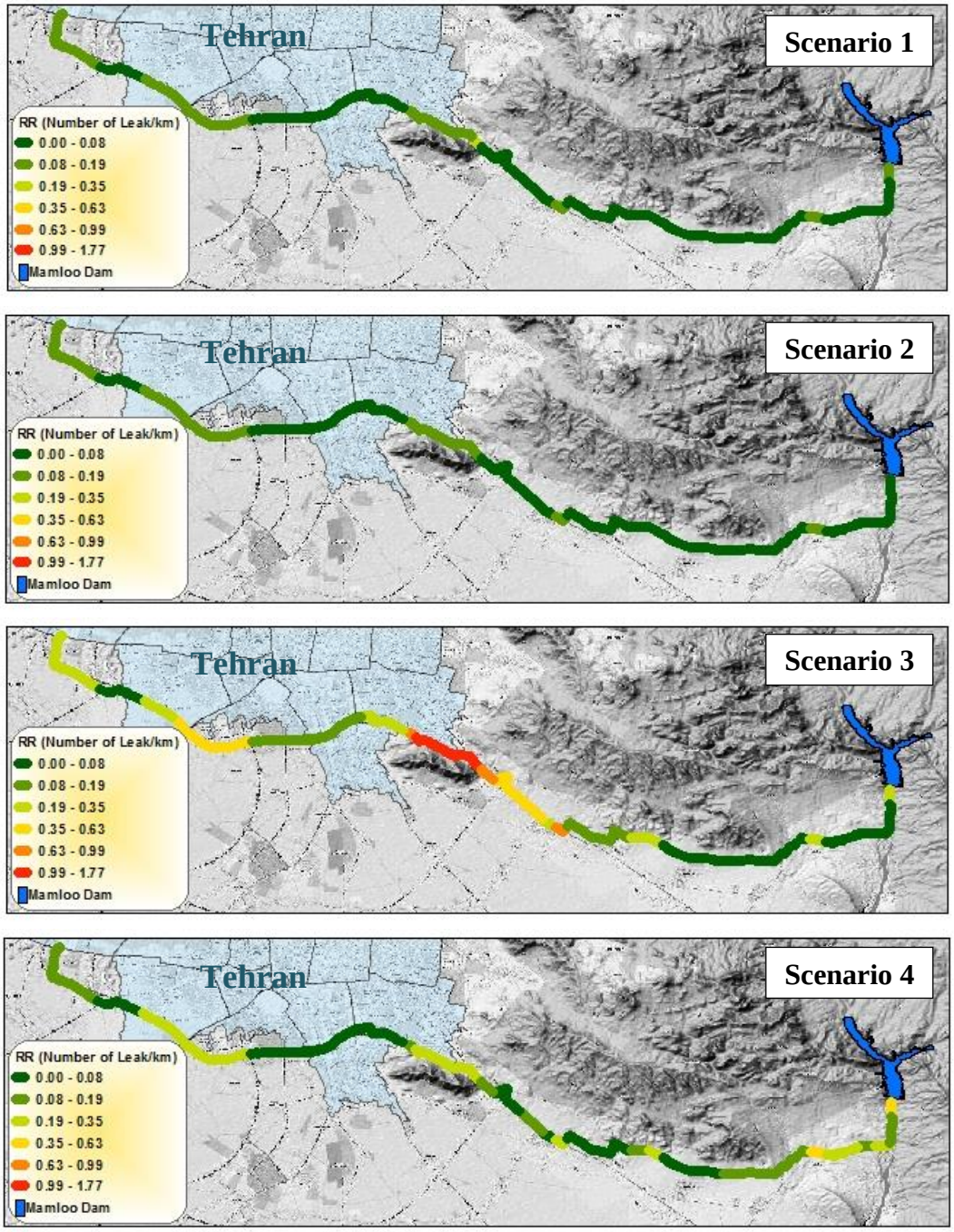

Fig. 6: The map of the number of leaks, for four different scenarios.

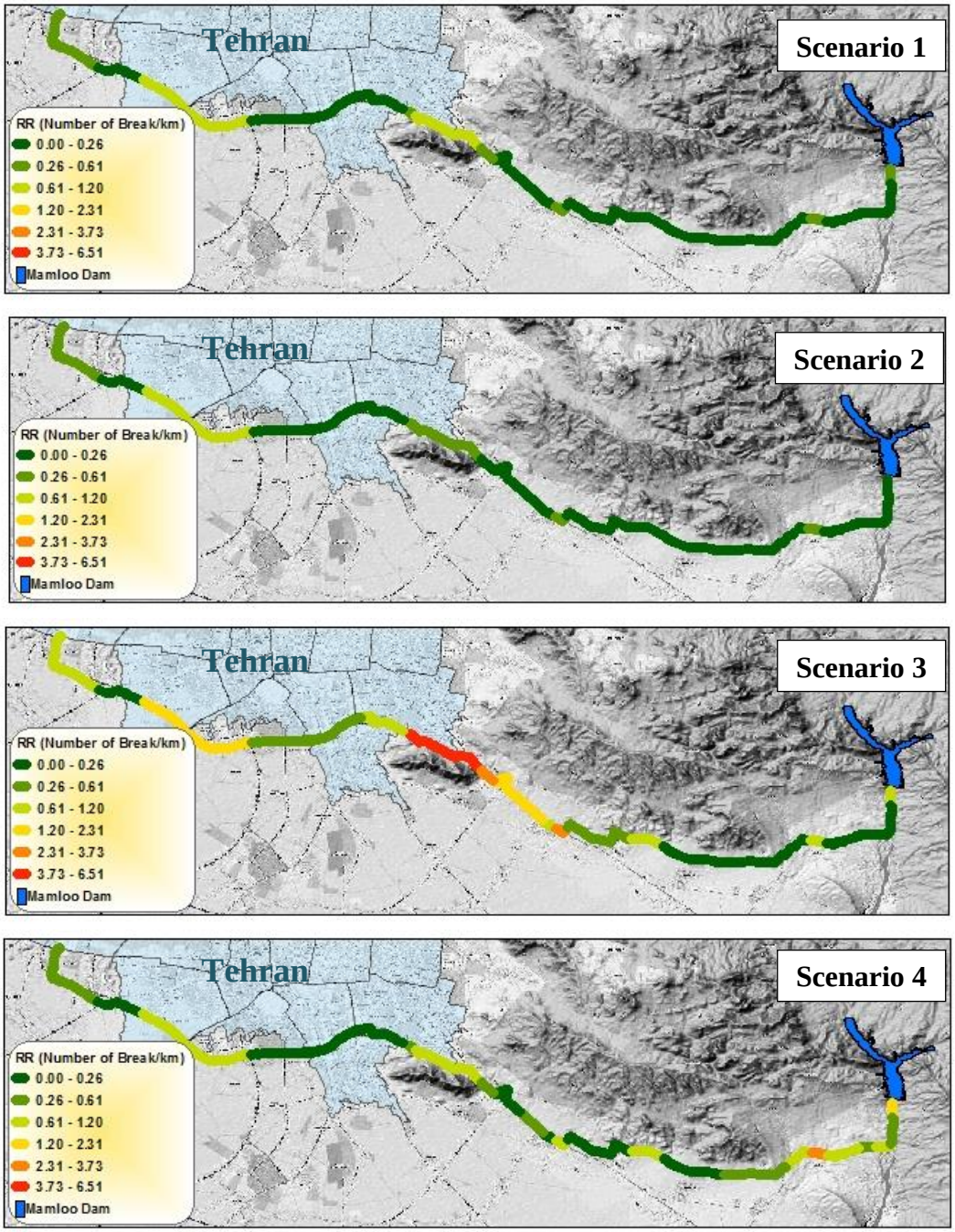

Fig. 7: The map of the number of breaks, for four different scenarios.

4. System Performance

4.1. Serviceability Evaluation

This section outlines the simplified methodology for a quick evaluation of the system's performance in the aftermath of an earthquake. This approach is based on system performance studies performed on the water network in Oakland, Tokyo, and San Francisco [14]. Based on these results, the damage algorithm proposed in this earthquake loss estimation for the simplified system performance evaluation is defined by a "conjugate" lognormal function (i.e., 1 - lognormal function). This damage function has a median of 0.1 repairs/km and a beta of 0.85, and is shown in Fig. 8. Hence, with the given knowledge of the pipe classification and length, one can estimate the system performance. That is, damage algorithms provided in the previous section evaluate repair rates and therefore the expected total number of repairs (i.e., by multiplying the predicted repair rate for each pipe type in the network by its length and summing up all pipes in the network) using Equations 6 and 7.

$$Number\ of\ leak = \sum_{j}^{m} \sum_{i}^{n} (RR_{leak})_{ij}\ L_i\ P_j \tag{6}$$

$$Number\ of\ break = \sum_{j}^{m}\sum_{i}^{n}(RR_{break})_{ij}\ L_i\ P_j \quad (7)$$

where m is the number of seismic hazards, n is the number of segment, $(RR)_{ij}$ is the repair rate of the i[th] segment due to j[th] hazard, L_i is the length of the i[th] segment, and P_j is the probability of j[th] hazard. The average repair rate is then computed as the ratio of the expected total number of repairs to the total length of pipes in the network by employing Eq. 8.

$$\text{Average break rate} = \frac{Number\ of\ break}{\sum L_i} \quad (8)$$

Hence, the serviceability index right after the earthquake is calculated using Equations 9, 10, and 11:

$$\text{SI} = 1 - \text{Lognormal}_{\text{Cumulative}}\ (\text{x: Average break rate, mean: Ln}(0.1), \text{S}_\text{D}\text{: } 0.85) \quad (9\text{-a})$$

or

$$\text{SI} = 1 - \text{Normal}_{Cumulative}\ (\text{x: } (\frac{\text{Ln}\left(\frac{\text{Average break rate}}{0.1}\right)}{0.85}), mean: 0, S_D: 0) \quad (9\text{-b})$$

$$\text{Normal}_{Cumulative}(x) = \frac{1}{2}[1 + \text{erf}(\frac{x}{\sqrt{2}})] \quad (10)$$

$$\text{erf}(z) = \frac{2}{\sqrt{\pi}}\int_0^z e^{-t^2}\,dt \quad (11)$$

According to the GIS-based analyses previously presented in Fig. 6 and 7, the total number of leaks and breaks due to liquefaction, landslide, and PGV for the considered scenarios are calculated and shown in Table 2. Also, the calculated average break rate and serviceability index are presented in Table 3.

Pipelines having poor earthquake resistance generally include old pipes and those susceptible to corrosion. Replacing old and vulnerable pipes with more seismically resistant and corrosion-resistant pipes reduces damage and can improve the post-earthquake network performance. Inadequate maintenance reduces the integrity and increases a facilities' vulnerability to earthquake damage. Therefore, providing adequate and continued maintenance for pipelines and other facilities helps safeguard against seismic damage. In this regard, a comparison is made between the current/initial performance of the studied pipeline (28% serviceability as presented in Table 4) and the updated performance after some hypothetical seismic improvements. As presented in Table 4 and Fig. 9, the water transmission pipeline's post-earthquake performance is considerably improved by implementing some seismic improvement efforts.

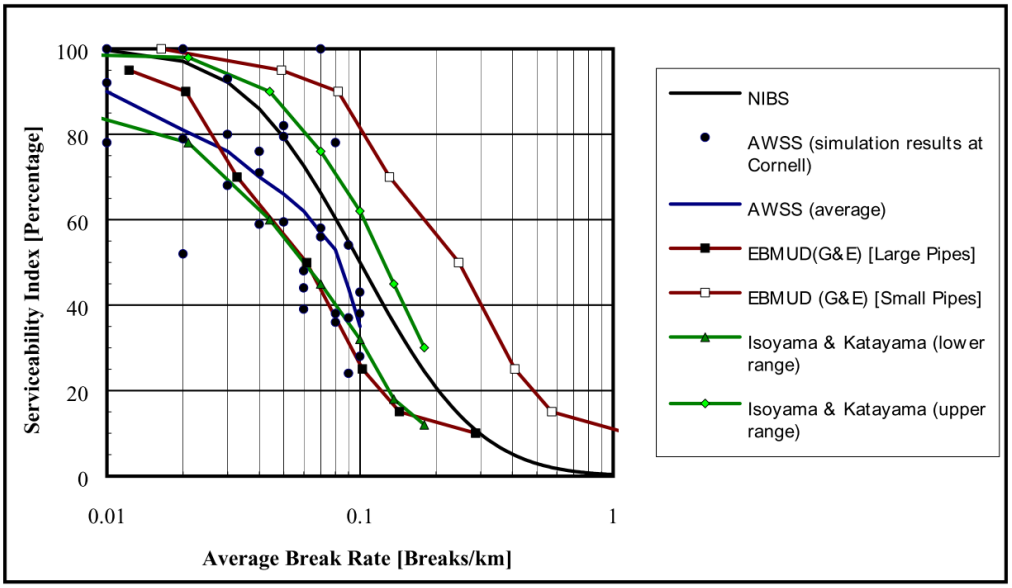

Fig. 8: Damage Index versus Average Break Rate for Post-Earthquake System Performance Evaluation [12].

Table 2. Number of leaks and breaks due to liquefaction, landslide, and PGV for four scenarios

Scenario	Number of the liquefaction-induced leak	Number of liquefaction-induced breaks	Number of the landslide-induced leak	Number of landslide-induced breaks	Number of PGV-induced leaks	Number of PGV-induced breaks
1	0.50	1.99	0.16	0.64	0.29	0.07
2	0.54	2.15	0.04	0.16	0.24	0.06
3	1.34	5.35	1.63	6.53	1.59	0.40
4	0.59	2.34	0.90	3.59	0.84	0.21

Table 3. Calculated average break rate and serviceability index

Scenario	Number of Total Leaks	Number of Total Breaks	Total Length	Average break rate	Serviceability index (%)
1	0.95	2.71	74.13	0.04	88.19
2	0.82	2.37	74.13	0.03	91.01
3	4.56	12.27	74.13	0.17	27.65
4	2.32	6.14	74.13	0.08	58.74

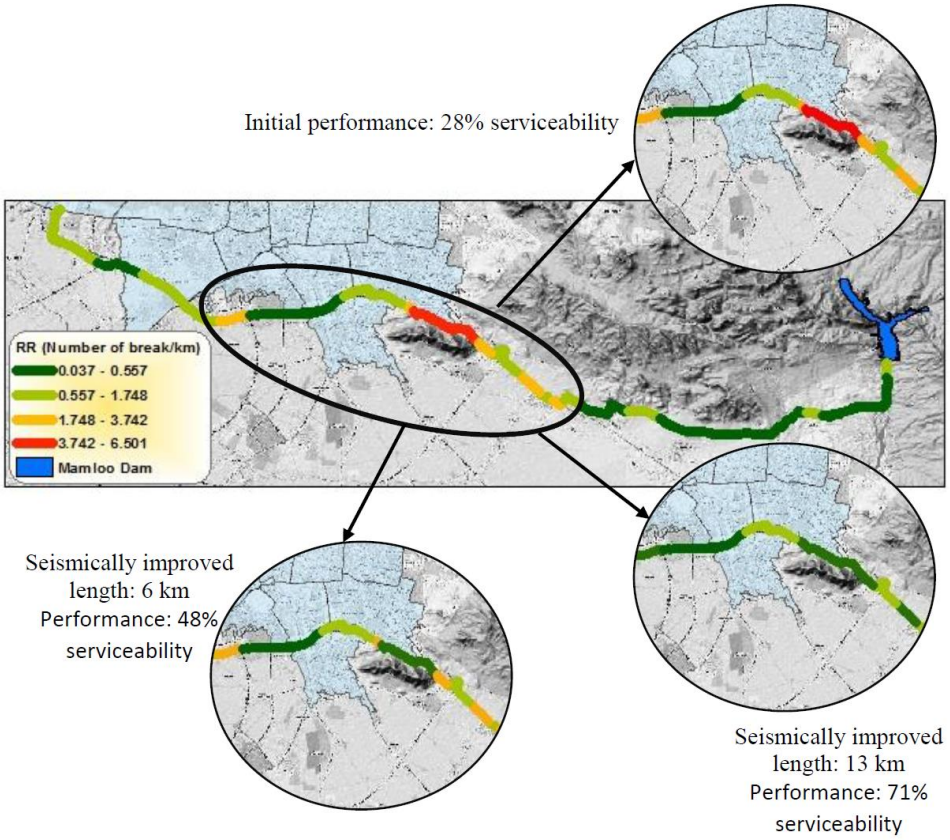

Fig. 9: Progressed serviceability of the studied pipeline regarding seismically performance improvement.

Table 4. Initial and updated serviceability index after seismic improvement

Seismically improved the length of the pipeline (km)	Number of Total Breaks	Total Length	Average break rate	Serviceability index (%)
0.00	12.27	74.13	0.17	28
6.00	7.66	74.13	0.10	48
13.00	4.62	74.13	0.06	71

4.2. Pipeline Restoration Analysis

As one of the main elements of the water infrastructure resilience model, understanding restoration time is critical for decision-makers and urban planners. It can improve the disaster resilience of cities in high-risk areas around the globe. The restoration functions for pipelines are expressed in terms of the number of days needed to fix the possible leaks and breaks. These restoration functions are given in Table 5.

Table 5. Restoration function for water pipelines [14]

Class	Diameter from: (in)	Diameter to: (in)	# Fixed Breaks per Day per worker	# Fixed Leaks per Day per worker	Priority
a	60	300	0.33	0.66	1 (Highest)
b	36	60	0.33	0.66	2
c	20	36	0.33	0.66	3
d	12	20	0.50	1.0	4
e	8	12	0.50	1.0	5 (Lowest)
u	Unknown diameter	or for Default Data Analysis	0.50	1.0	6 (Lowest)

Where the user can specify the total number of available workers, it should be noted that the values in Table 5 are based on the following assumptions:

1. Pipes that are less than 20" in diameter are defined as small, while pipes with a diameter greater than 20" are defined as large."
2. For both small and large pipes, a 16-hour daily shift is assumed.
3. For small pipes, a 4-person crew needs 4 hours to fix a leak, while the same 4-person crew needs 8 hours to fix a break. (Mathematically, this is equivalent to saying it needs 16 people to fix a leak in one hour and it needs 32 people to fix a break in one hour).
4. For large pipes, a 4-person crew needs 6 hours to fix a leak, while the same 4-person crew needs 12 hours to fix a break. (Mathematically, this is equivalent to say it requires 24 people to fix a leak in one hour and 48 people to fix a break in one hour).

With this algorithm for potable water pipelines, the total number of days needed for quality repairs is calculated using Eq. 12:

Days needed to finish all repairs = (1/available worker) * [(# small pipe leaks/1.0) + (# small pipe breaks/0.5) + (# large pipe leaks/0.66) + (# large pipe breaks/0.33)] (12)

According to the above-mentioned consideration and also regarding the rough average of 247000 cubic meters of water transmitted per day utilizing the studied pipeline, the backup water resources needed during the repair process are evaluated. After that, the number of workers needed to accomplish all repairs at a particular time can be calculated by employing Fig. 10 and assuming the backup water resources. It is worth noting that Fig. 10 is produced regarding the worst earthquake scenario (when the Rey fault is activated), which causes the least serviceability index of 27.65%. For example, as shown in Fig. 10, if the backup resources save 2.1 million cubic meters of water with a crew size of 5, it can then be expected that nine days is needed to finish all repairs according to the Rey fault activation scenario.

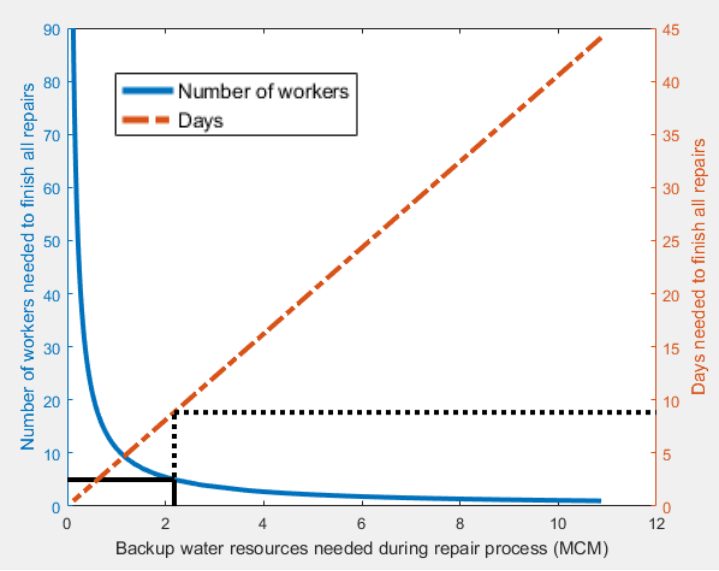

Fig. 10: Restoration curve for the worst scenario (Rey fault activation).

It is understood that the overall resilience increases while the number of impacted customers reduces. Although the time required for total system recovery may be reduced by implementing some seismic improvement efforts, a forecast of the crews needed to ensure adequate response and recovery is required; this can be facilitated using the results of damage estimates explained before to complete repairs needed and to meet the performance criteria. It is important to note that if the crews maintained for routine operations are not adequate to meet the performance criteria, additional teams may be necessary. Since it is yet generally difficult to justify sustaining additional crews in preparation for an emergency, seismic improvements should be performed to reduce the crew size, alternatively. Hence, a reliable estimation about what will happen after a probable earthquake must be made, similar to what is done in the current study, to evaluate the post-earthquake resilience of the water transmission systems. Such studies can provide useful information for the decision maker and responsible authorities to plan for mitigating the probable damages due to the predicted seismic hazard level.

5. Conclusion

Infrastructure has always played an important role in the seismic resilience of urban regions. Water transmission systems are considered vital infrastructure; they should hence be rigorously assessed as to whether they can keep their functionality if subjected to seismic loads, and they sustain damage, how long it would take for their recovery process. As earthquake events are often followed by several consequences, a rigorous investigation should include not only the earthquake itself but also its consequences such as landslides, liquefaction, fault movement, etc. To meet this aim, a macro-scale study employing GIS is needed whereby potential earthquake and post-earthquake damage can be predicted; required mitigation strategies can hence be adopted in advance. This research aimed at analyzing Tehran's southern water transmission system subject to the earthquake and post-earthquake events. This research demonstrates the vital importance of urban resilience features, recovery time, and functional recovery teams to increase urban water system resilience. Results indicated that in the worst potential earthquake (Rey fault activated), water transmission systems would suffer more than 72% of the service disruption just after the probable earthquake, which means 28% of the system serviceability would exist. This article also made a comparison to depict how performing some seismic improvements in the most vulnerable segments of the pipeline can enhance the system serviceability. Results show that retrofitting and improving the 6 km and 13 km of the pipeline's vulnerable length will increase the serviceability to 48% and 71%, respectively.

References:

[1] Roohi, M., et al., *Implication of building inventory accuracy on physical and socio-economic resilience metrics for informed decision-making in natural hazards*. Structure and Infrastructure Engineering, 2020. 17(4): p. 534-554.

[2] Maghsoudi-Barmi, A., et al., *Probabilistic seismic performance assessment of optimally designed highway bridge isolated by ordinary unbonded elastomeric bearings.* Engineering Structures, 2021. 247: p. 113058.

[3] Khansefid, A. *Lifetime risk-based seismic performance assessment of buildings equipped with supplemental damping and base isolation systems under probable mainshock-aftershock scenarios*. in *Structures*. 2021. Elsevier.

[4] Fallahi, A., H. Zafari, and A. Bakhtiari, *Urban areas and reduce the risk of injury*, in *Fifth International Conference on Seismology and Earthquake Engineering*. 2007: International Institute of Seismology and Earthquake Engineering: Tehran, Iran. p. 92–99.

[5] Eskandari, M., et al., *Geospatial analysis of earthquake damage probability of water pipelines due to multi-hazard failure*. ISPRS International Journal of Geo-Information, 2017. 6(6): p. 169.

[6] Mousavi, M., M. Hesari, and A. Azarbakht, *Seismic risk assessment of the 3rd Azerbaijan gas pipeline in Iran.* Natural hazards, 2014. 74(3): p. 1327-1348.

[7] Farahani, S., A. Tahershamsi, and B. behnam, *Earthquake and post-earthquake vulnerability assessment of urban gas pipelines network.* Natural Hazards, 2020.

[8] Farahani, S., B. Behnam, and A. Tahershamsi, *Probabilistic seismic multi-hazard loss estimation of Iran gas trunklines.* Journal of Loss Prevention in the Process Industries, 2020: p. 104176.

[9] Taylor, C.E. *Seismic Loss Estimates for a Hypothetical Water System: A Demonstration Project*. 1991. ASCE.

[10] Katayama, T., *EARTHQUAKE DAMAGE TO WATER AND GAS DISTRIBUTION SYSTEMS.* 1975.

[11] O'Rourke, M. and G. Ayala, *Pipeline damage due to wave propagation*. Journal of Geotechnical Engineering, 1993. 119(9): p. 1490-1498.

[12] FEMA, *Multi-Hazard Loss Estimation Methodology, Earthquake Model, HAZUS-MH2. 1*. 2012: Washington, D.C.

[13] O'Rourke, T., S. Toprak, and Y. Sano. *Factors affecting water supply damage caused by the Northridge earthquake*. in *US-Japan Workshop on Earthquake Disaster Prevention For Lifeline Systems*. 1998.

[14] ALA, *American Lifeline Alliance, Seismic fragility formulations for water systems, Part I-Guideline. Reston, VA: ALA.* 2001.

[15] Pineda-Porras, O. and M. Ordaz-Schroeder, *Seismic vulnerability function for high-diameter buried pipelines: Mexico City's primary water system case*, in *New pipeline technologies, security, and safety*. 2003. p. 1145-1154.

[16] Ayala, A.G. and M.J. O'Rourke, *Effects of the 1985 Michoacan earthquake on water systems and other buried lifelines in Mexico.* 1989.
[17] Rahnama, R., et al., *Study of Seismic Vulnerability for Retrofitting Water Supply Network of Tehran District 11*. Disaster Prevention and Management Knowledge (quarterly), 2016. **5**(4): p. 308-314.
[18] Sabeti, R., S. Jamali, and H.H. Jamali, *Simulation of thermal stratification and salinity using the Ce-Qual-W2 model (case study: mamloo dam).* Engineering, Technology & Applied Science Research, 2017. **7**(3): p. 1664-1669.
[19] Vernant, P., et al., *Present-day crustal deformation and plate kinematics in the Middle East constrained by GPS measurements in Iran and northern Oman.* Geophysical Journal International, 2004. 157(1): p. 381-398.
[20] Masson, F., et al., *Strain rate tensor in Iran from a new GPS velocity field.* Geophysical Journal International, 2014. 197(1): p. 10-21.
[21] Khorrami, F., et al., *An up-to-date crustal deformation map of Iran using integrated campaign-mode and permanent GPS velocities.* Geophysical Journal International, 2019. 217(2): p. 832-843.
[22] Talebian, M., et al., *Active faulting within a megacity: the geometry and slip rate of the Pardisan thrust in central Tehran, Iran.* Geophysical Supplements to the Monthly Notices of the Royal Astronomical Society, 2016. 207(3): p. 1688-1699.
[23] Hessami, K. and F. Jamali, *Explanatory notes to the map of major active faults of Iran.* Journal of Seismology and Earthquake Engineering, 2020. 8(1): p. 1-11.
[24] JICA, C., *The study on seismic microzoning of the Greater Tehran Area in the Islamic Republic of Iran.* Pacific Consultants International Report, OYO Cooperation, Japan, 2000: p. 291-390.
[25] Farahani, S., B. Behnam, and A. Tahershamsi, *Macrozonation of Seismic Transient Ground Displacement and Permanent Ground Deformation of Iran.* Nat. Hazards Earth Syst. Sci. Discuss., 2020. 2020: p. 1-20.
[26] Wald, D., et al., *ShakeMap manual: technical manual, user's guide, and software guide: US Geological Survey*. Techniques and Methods TM12-A1, 2005. 132.
[27] Allen, T. and D. Wald, *Topographic Slope as a Proxy for Seismic Site-Conditions (Vs30) and Amplification Around the globe. Open-File Report 2007–1357*. US Geological Survey, Reston, Virginia, 2007.
[28] Komakpanah, A. and M. Farajzadeh. *Liquefaction susceptibility and opportunity macrozonation of Iran*. in *Second international conference on seismology and earthquake engineering*. 1995. Tehran, Iran.
[29] Sadigh, K., J. Egan, and R. Youngs, *Specification of ground motion for seismic design of long period structures.* Earthquake notes, 1986. 57(1): p. 13.
[30] Tokimatsu, K. and H.B. Seed, *Evaluation of settlements in sands due to earthquake shaking.* Journal of geotechnical engineering, 1987. 113(8): p. 861-878.
[31] GSI, *Geological Survey and Mineral Explorations of Iran (GSI)*, http://gis.ir. 2018.
[32] Makdisi, F.I. and H.B. Seed, *Simplified procedure for estimating dam and embankment earthquake-induced deformations.* Journal of Geotechnical and Geoenvironmental Engineering, 1978. 104(Proceeding): p. 849-867.